This is an Accepted Manuscript version of the following article, accepted for publication in JOURNAL OF THERMAL STRESSES.
Postprint of: Igumnov L., Volkov I., Kazakov V., Shishulin D., Modin I., Belov A., Eremeev V., Experimental and theoretical study on high-temperature creep of VT6 titanium alloy under multi-axial loading conditions, JOURNAL OF THERMAL STRESSES, Vol. 47, iss. 6 (2024), pp. 727-742, DOI: 10.1080/01495739.2024.2340602
It is deposited under the terms of the Creative Commons Attribution-NonCommercial License (http://creativecommons.org/licenses/by-nc/4.0/), which permits non-commercial re-use, distribution, and reproduction in any medium, provided the original work is properly cited.

Experimental and theoretical study on high-temperature creep of VT6 titanium alloy under multi-axial loading conditions

Leonid A. Igumnov[a], Ivan A. Volkov[a,b], Dmitrii A. Kazakov[a], Denis N. Shishulin[a], Ivan A. Modin[a,b], Aleksandr A. Belov[a], and Victor A. Eremeyev[c,d]

[a]Research Institute for Mechanics, National Research Lobachevski State University of Nizhny Novgorod, Nizhny Novgorod, Russian Federation; [b]Volga State University of Water Transport, Nizhny Novgorod, Russian Federation; [c]Department of Mechanics of Materials and Structures, Faculty of Civil and Environmental Engineering, Gdansk University of Technology, Gdansk, Poland; [d]Department of Civil and Environmental Engineering and Architecture (DICAAR), University of Cagliari, Cagliari, Italy

ABSTRACT

In the framework of damage mechanics, we discuss a new mathematical model that describes the kinetics of the stress–strain state and damage accumulation during material degradation by the mechanism of long-term strength under complex multiaxial stress state. An experimental and theoretical technique is proposed for determination of material parameters and scalar constitutive functions for damaged media based on specially set experiments on laboratory specimens. The results of experimental studies and numerical simulations of short-term high-temperature creep of VT6 titanium alloy under uniaxial and multiaxial loading are presented. Numerical results are compared with the data obtained through experiments. Particular attention is paid to simulating the process of unsteady creep for complex deformation modes, accompanied by rotation of main areas of stress, strain and creep strain tensors. It is shown that the developed version of the constitutive relations of the damaged media enables us to describe the processes of unsteady creep and long-term strength of structural alloys under multiaxial stress with the accuracy sufficient for engineering calculations.

1. Introduction

The key feature of structural elements undergoing failure under high-temperature creep is non-stationary nature of thermal and force actions that determine the nature of material deformation in the zones of stress concentration at different time duration, stress levels and temperatures [1–6].

Numerous experimental results indicate that the nature of failure under thermo cyclic loading at various cycle times differs due to the difference in combinations of two main types of damage: the damage caused by the creep that develops mainly along the grain boundaries (inter granular fracture) and the damage caused by plastic deformation along the slip planes of dislocations (transcrystalline fracture).

Since the processes of damage accumulation depend on the kinetics of the stress–strain state (SSS), the accuracy of strength and service life assessment of structural elements will depend on reliability of a mathematical model of the mechanics of damaged media (MDM) in describing

deformation processes in hazardous zones of structural elements under specified operating conditions and on the accuracy in determining material parameters within mathematical model.

The service life of structural elements subjected to elevated temperatures and to cyclic mechanical loads is mainly determined by the physical processes of low cycle fatigue (LCF) and damage accumulation due to creep, which lead to one of the most dangerous types of failure - brittle fracture of structures originally made from plastic materials.

Many simplified one-dimensional constitutive equations have been proposed to describe the standard creep curves. However, they are suitable only for the case of constant stresses and represent an attempt to mathematically formalize the first and second stages of creep process [7–14].

The models of temporary and strain hardening under alternating stresses were developed [7, 10]. However, the constitutive creep relations presented in the form of temporary and strain hardening models are intended only to describe the first and second stages of creep process. They neither cover all stages of creep process nor describe the important phenomenon of reverse creep during material unloading. Therefore, in a number of cases it is necessary to formulate more complex constitutive relations for creep and long-term strength [15–21]. A large number of various formulations of creep models have been proposed by domestic and foreign researchers [2, 10]. However, there is an opinion shared by many researchers that relations based on the generalization of hardening models by applying the concept of "hidden" or "internal" state parameters may agree satisfactory for engineering calculations with experimental data under multiaxial stress states. Such relations have two important advantages: they cover a wide range of material behavior including determination of scleronomous plastic deformation and rheonomious creep, and at the same time they are very convenient for analyzing effective stresses.

Particular attention should be paid to experimental studies of high-temperature creep under multiaxial loading, since these experimental data are the basis for constructing a reliable mathematical model, which allows to take into account the effects arising from complex disproportionate loads and significantly affecting the accuracy of calculations of long-term structural strength.

This paper presents experimental studies of short-term high-temperature creep of VT6 titanium alloy under uniaxial and multiaxial stress states. A mathematical model of MDM is developed to describe the processes of unsteady creep and long-term strength of polycrystalline structural alloys based of the works of domestic and foreign researchers [6, 15–21].

The reliability of the developed constitutive relations of MDM was assessed by comparing the experimental results with calculated data on the short-term high-temperature unsteady creep of the VT6 titanium alloy under uniaxial and multiaxial stresses.

2. Experimental equipment and test program

The capabilities of the testing equipment [4, 22–24] with integrated software allow you to create ·ious programs for testing laboratory samples of the corresponding geometry. The results of ɔerimental studies of laboratory specimens of VT6 titanium alloy for short-term high-tempera-·e creep under uniaxial and multiaxial stress state are given below. Laboratory specimens con-ted of a hollow tube with an outer diameter of $d = 16 \pm 0.05$ mm and a wall thickness of $= 1 \pm 0.05$ mm made of VT6 titanium alloy with a working part length of 80 mm (Figure 1). e shape and size of the specimen under tension and torsion ensured a uniform distribution of · stress and strain fields in the working part of the specimen. The tests were carried out on a iversal test complex Z100 ZWICK-ROEL (Germany), which allows you to conduct experiments complex multiaxial loading in a quasistatic range of strain rates with a simultaneous, time-ıchronized setting of the following parameters: rate of change in the longitudinal force (or dis-.cement); rate of change in torque (or twist angle); rate of change in the internal pressure. The ıiting values of the parameters are ± 100 kN by force, ± 1000 Nm by torque, and − 0 to MPa by pressure. The measuring equipment of the complex includes a transverse strain meter

MOST WIEDZY Downloaded from mostwiedzy.pl

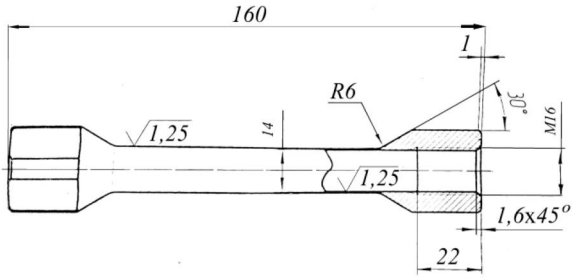

Figure 1. View of laboratory specimen.

Figure 2. A General view of the testing setup Z100 ZWICK-ROEL.

based on a ME46 video extensometer with a resolution of 0.4–2 μm, a LaserXtens laser extensometer that can simultaneously measure both longitudinal deformations (measuring base 20–100 mm) with a resolution of $\leq$ 1 μm and deformations at torsion, ISO 9513 accuracy class1, force transducer 0–250 kN, ISO 7500-1 accuracy class1.

The unit is equipped with an EC 2181 heat chamber with a controller which allows to test ious types of specimens in the temperature range from minus 150 to plus 600 °C. A general w of the setup is shown in Figure 2. To conduct tests, the experimental setup was configured conduct high-temperature creep experiments taking into account the main required test condins—rigid, clearance-free fixing of specimens in the grips of the loading device and test control shock-free transitions from one loading mode to another. A uniform temperature distribution the working part of the specimen was ensured by using a heat chamber with forced convecn and temperature control directly on the laboratory specimen.

The creep of VT6 titanium alloy was experimentally studied according to the soft loading ıeme at a temperature of 600 °C under uniaxial loading (torsion (Figure 3a,b) with stress intenes σ_u= 50 and 66 MPa, extension (Figure 3c–f), with stress intensities σ_u= 30, 66, 78 and MPa and multiaxial loading with two levels of stress intensity σ_u= 50 and 78 MPa at angles ween the components of the stress tensor σ_{11} and $\sqrt{3}\sigma_{12}$ equal to 30° and 60°, respectively

MOST WIEDZY Downloaded from mostwiedzy.pl

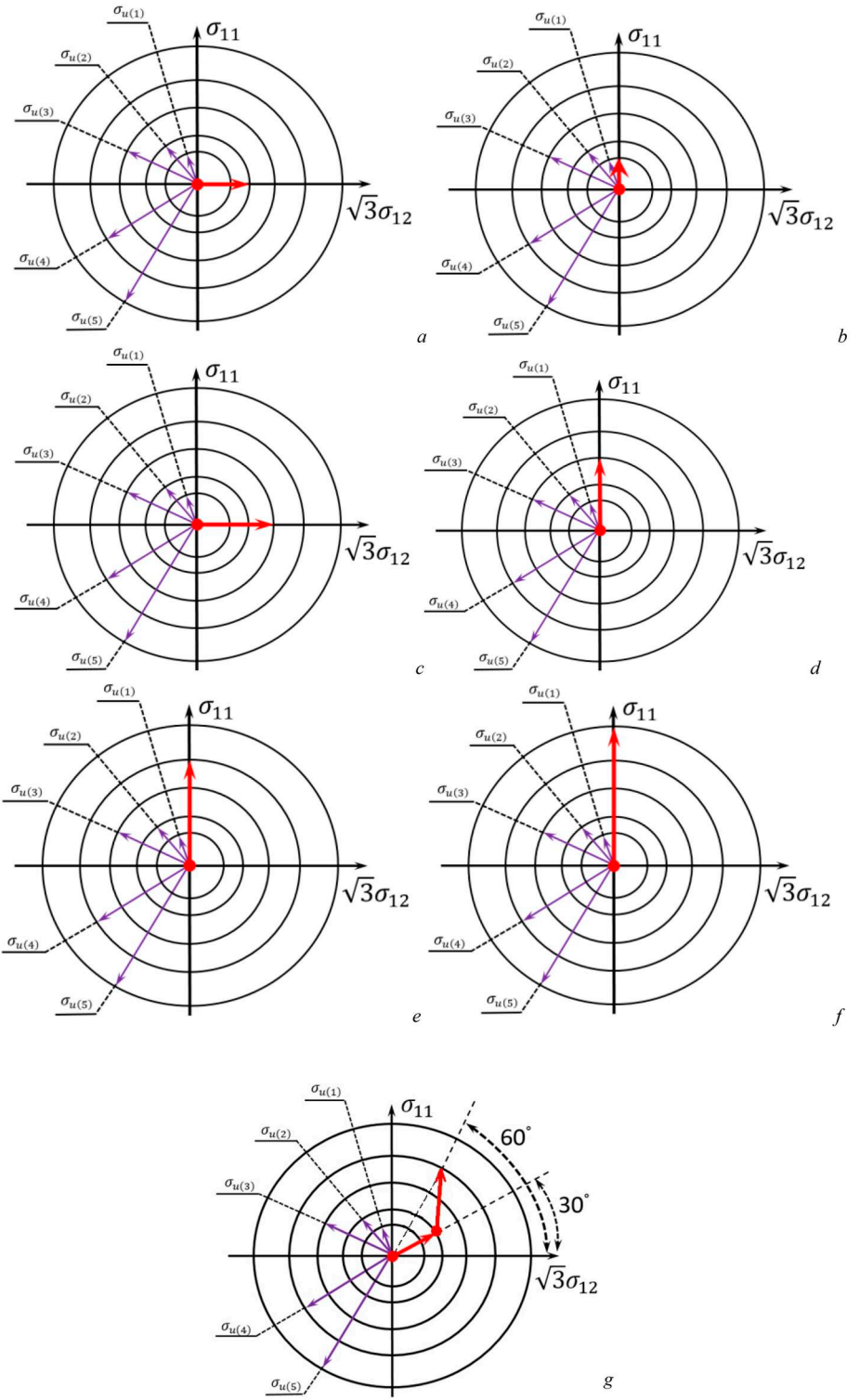

ure 3. The loading program for laboratory specimens in the stress space.

MOST WIEDZY Downloaded from mostwiedzy.pl

(Figure 3g). Figure 3 shows the loading program, where the red arrow indicates the vector of the effective stress in experimental studies of the creep process and the indicated circle radii are equal to the following values $\sigma_{u(1)} = 30$ MPa, $\sigma_{u(2)} = 50$ MPa, $\sigma_{u(3)} = 66$ MPa, $\sigma_{u(4)} = 78$ MPa, $\sigma_{u(5)} = 90$ MPa.

Based on the results of experimental studies, creep curves were constructed—creep strains as a function of time $e^c{}_{11}(t), e^c{}_{12}(t)$ for the above loading laws (Figures 7–14).

3. Constitutive relations of non-stationary creep

The model of damaged medium for describing the degradation of initial strength properties by the long-term strength mechanism, consists of three interrelated parts:

- Relations defining viscoplastic behavior of the material with account for its dependence on failure process;
- Evolutionary equations describing the kinetics of damage accumulation;
- Strength criterion for damaged material.

3.1. Constitutive relations of thermal creep

To estimate the creep process, a mathematical model is used in which the variation laws of internal parameters of the material are assumed to be determined by two physical mechanisms: hardening and softening of materials. This approach has an analogue in the mathematical theory of plasticity (flow theory).

The main provisions of the used version of non-stationary creep relations proposed by Korotkikh and developed in the works of his students are as follows [6, 21, 25,26]:

1. Initially isotropic media are considered.
2. The strain and strain rate tensors are the sum of the "instantaneous" and "temporary" components. The "instant" component consists of elastic components that are independent of the history of deformation and determine the final state of the process, and plastic components that depend on the history of the deformation process. The time component (creep strain) describes time-dependent deformation processes under low loading rates.
3. The evolution of the equipotential creep surface is described by a change in its radius C_c and by displacement of it is center $\rho^c{}_{ij}$.
4. The change in the volume of the body element is elastic, i.e. $e^p{}_{ij} = e^c{}_{ij} = 0$.
5. The processes of deformation characterized by small deformations are considered.

It is assumed that the components of the strain tensor e_{ij} and their rates $\dot{e}_{ij}$ are the sums of stic components $e^e{}_{ij}, \dot{e}^e{}_{ij}$, plastic components $e^p{}_{ij}, \dot{e}^p{}_{ij}$, creep deformations $e^c{}_{ij}, \dot{e}^c{}_{ij}$, i.e.,:

$$e_{ij} = e_{ij}{}^e + e_{ij}{}^p + e_{ij}{}^c, \ \dot{e}_{ij} = \dot{e}_{ij}{}^e + \dot{e}_{ij}{}^p + \dot{e}_{ij}{}^c, \ i, \ j = 1, 2, 3. \tag{1}$$

The relationship between the stress tensor and elastic strain tensor is determined as in the case thermoelasticity:

$$\sigma = 3K[e - \alpha T], \dot{\sigma} = 3K[\dot{e} - \dot{\alpha} T - \alpha \dot{T}] + \frac{\dot{K}}{K}\sigma. \tag{2}$$

$$\sigma'_{ij} = 2Ge'_{ij}{}^e, \dot{\sigma}_{ij} = 2G\dot{e}_{ij}{}^e + \frac{\dot{G}}{G}\sigma'_{ij}, e'_{ij}{}^e = e'_{ij} - e_{ij}{}^c - e_{ij}{}^p \tag{3}$$

ere σ, e are spherical and σ'_{ij}, e'_{ij} are deviator components of the corresponding stress σ_{ij} and

MOST WIEDZY Downloaded from mostwiedzy.pl

strain e_{ij}, respectively; $G(T)$ is the shear modulus; $K(T)$ is the volumetric compression modulus; $\alpha(T)$ is the coefficient of temperature expansion.

To describe the creep processes, we introduce in the stress space the equipotential creep surfaces F_c, which have the common center $\rho^c{}_{ij}$ and different radii C_C, defined by the current stress state:

$$F_c^{(i)} = S_{ij}^c S_{ij}^c - C_c^2 = 0, S_{ij}^c = \sigma'_{ij} - \rho_{ij}^c, \quad i = 0, 1, 2, \ldots \tag{4}$$

In accordance with the associativity law

$$\dot{e}_{ij}^c = \lambda_c \frac{\partial F_c^{(i)}}{\partial S_{ij}^c} = \lambda_c S_{ij}^c \tag{5}$$

where λ_c corresponds to the current surface $F^{(i)}{}_c$, defining the current stress state $S_{ij}{}^c$. The surface with radius $\bar{C}_c$ may be outlined among these equipotential surfaces as corresponding to zero creep rate:

$$F_c^{(0)} = \bar{S}_{ij}^c \bar{S}_{ij}^c - \bar{C}_c^2 = 0, \bar{S}_{ij}^c = \overline{\sigma'}_{ij} - \rho_{ij}^c \tag{6}$$

where $\bar{S}_{ij}{}^c$ and $\overline{\sigma'}_{ij}$ are the set of stress states corresponding (to a certain tolerance) to the zero creep rate, C_c is experimentally determined function of temperature T and χ_c.

$$\dot{\chi}_c = \sqrt{\frac{2}{3}\dot{e}_{ij}^c \dot{e}_{ij}^c}, \chi_c = \int_0^y \dot{\chi}_c dt \tag{7}$$

The evolution equation for the change in the coordinates of the creep surface center has the form [15, 27]:

$$\dot{\rho}_{ij}^c = g_1^c \dot{e}_{ij}^c - g_2^c \rho_{ij}^c \dot{\chi}_c + g^c{}_3(T) \tag{8}$$

where $g_1{}^c$ and $g_2{}^c > 0$ are experimentally determined material parameters.

By specifying (3), the law of gradientality can be represented in the following form:

$$\dot{e}^c{}_{ij} = \lambda_c(\psi_c, T) S_{ij}^c = \lambda_c \psi_c S_{ij}^c = \lambda_c \frac{\sqrt{S_{ij}^c S_{ij}^c} - C_c}{C_c} \tag{9}$$

$$\psi_c = \frac{\sqrt{S_{ij}^c S_{ij}^c} - \bar{C}_c}{C_c} \tag{10}$$

In expression (9), λ_c is experimentally determined function equal to zero at $\psi_c \leq 0$. The length of the creep strain path will take the form:

$$\dot{\chi}_c = \sqrt{\frac{2}{3}} \lambda_c \left(\sqrt{S_{ij}^c S_{ij}^c} - \bar{C}_c \right) \tag{11}$$

The dependence χ_c on timetat $S_u^c = const$ in the case of multi-axial deformation over the ray jectory has the form presented in Figure 4.

The curve $\chi_c(t)$ can be conventionally divided into three segments:

The segment of unsteady creep from 0 to $\chi^{(1)}{}_c$, where the creep strain rate $\dot{\chi}_c$ decreases;
The segment of steady creep from $\chi^{(1)}{}_c$ to $\chi^{(2)}{}_c$, where the creep strain rate $\dot{\chi}_c$ is approximately constant, ($\dot{\chi}_c \cong const$);
The segment of unsteady creep $\chi_c > \chi^{(2)}{}_c$, where the creeps trains grow quickly (the segment to failure), $\dot{\chi}_c$ drastically increases.

Downloaded from mostwiedzy.pl
MOST WIEDZY

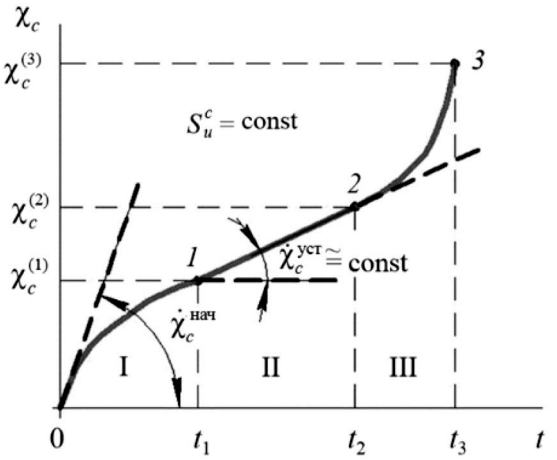

Figure 4. Generalized creep curve.

The lengths of these segments depend on the value S_u^c.

In the case of multiaxial loading we have:

$$\lambda_c = \begin{cases} 0, \psi \le 0 \cup \chi_c = 0, \\ \lambda_c^I, 0 \le \chi_c \le \chi^{(1)}{}_c, \\ \lambda_c^{II}, \chi^{(1)}{}_c \le \chi_c \le \chi^{(2)}{}_c, \\ \lambda_c^{III}, \chi^{(2)}{}_c \le \chi_c \le \chi^{(3)}{}_c. \end{cases} \tag{12}$$

The equation for $\lambda_c{}^I$ on the first segment of creep curve can be represented in the form:

$$\lambda_c^I = \lambda_c^{(0)}\left(1 - \frac{\chi_c}{\chi_c^{(1)}}\right) + \lambda_c^{(II)}\frac{\chi_c}{\chi_c^{(1)}} \tag{13}$$

At the stage of active development and merging of defects scattered over the volume of the material, the effect of the damage degree on the physical–mechanical characteristics is observed. In a first approximation, this effect can be described based on the concept of a degrading continuum by introducing effective stresses [6, 14]:

$$\tilde{\sigma}'_{i\ j} = F_1(\omega)\sigma'_{i\ j} = \frac{G}{\tilde{G}}\sigma'_{i\ j}\ \ \tilde{\sigma} = F_2(\omega)\sigma = \frac{\mathrm{K}}{\tilde{\mathrm{K}}}\sigma. \tag{14}$$

are effective module of elasticity determined by McKenzie formulas [6]:

$$\tilde{G} = G(1-\omega)\left[1 - \frac{(6K+12G)}{(9K+8G)}\omega\right], \tilde{K} = 4GK(1-\omega)/(4G+3K\omega) \tag{15}$$

Effective micro stress tensor $\tilde{\rho}_{ij}^c$ is determined in a similar way:

$$\tilde{\rho}_{ij}^c = F_1(\omega)\rho_{ij}^c = \frac{G}{\tilde{G}}\rho_{ij}^c. \tag{16}$$

?. Evolutionary equation of damage accumulation

e postulate that the evolutionary equation of damage accumulation under creep can be repre-ıted in the following form [14, 28]:

$$\dot{\omega} = f_1(\beta)f_2(\omega)f_3(W_c)f_4\left(\dot{W}_c\right). \tag{17}$$

MOST WIEDZY Downloaded from mostwiedzy.pl

where $f_1(\beta)$ is dominant function of volumetric stress strain state; $f_2(\omega)$ is dominant function of the level of accumulated damage; $f_3(W_c)$ is accumulated relative energy of damage spent on microdefect nucleation; $f_3(\dot{W}_c)$ is the function of the rate of change of the energy spent on microdefect formation introduced as follows

$$f_1(\beta) = \exp(k\beta) \tag{18}$$

$$f_2(\omega) = \begin{cases} 0, & W_c \le W_c^a \\ \omega^{\frac{1}{3}}(1-\omega)^{\frac{2}{3}}, & W_c > W_c^a \quad \omega \le \dfrac{1}{3} \\ \sqrt[3]{16}\dfrac{}{9}\omega^{-\frac{1}{3}}(1-\omega)^{-\frac{2}{3}}, & W_c > W_c^a \quad \omega > \dfrac{1}{3} \end{cases}$$

$$f_3(W_c) = \frac{W_c - W_c^a}{W_c^f}$$

$$f_4(\dot{W}_c) = \dot{W}_c / W_c^f$$

$$\dot{W}_c = \rho_{ij}^c \dot{e}_{ij}^c, \quad W_c = \int_0^t \dot{W}_c dt$$

Here $\beta = \sigma/\sigma_u$ is volumetric parameter of stress strain state, W_c^a is the value of damage energy at the end of the nucleation stage of micro defects scattered over the volume of the material, W_c^f is the value of the energy corresponding to a macro crack nucleation and k is material parameter. The evolutionary equation of damage accumulation (17) includes two-stage kinetics of damage accumulation scattered over the volume: the first stage is nucleation and growth of micro defects, the second stage is merging and further growth of micro defects with a significant damage effect on physical–mechanical properties of the material.

3.3. Strength criterion for damaged material

The condition when damage reaches its critical value is taken as a criterion of the end of the development phase of scattered micro defects:

$$\omega = \omega_f \le 1. \tag{19}$$

4. Determination of thermal creep parameters

For practical application of thermal creep equations (1)–(9), it is necessary to have the following data:

Dependencies $G(T)$, $K(T)$, $\alpha(T)$ on temperature T;
Dependence of the current radius of zero level creep surface (zero creep rate) $\bar{C}_c = \bar{C}_c(\chi_c, T)$ on T
Dependences of parameters $\lambda_c^{(0)} = \lambda_c^{(0)}(T)$ and $\lambda_c^{(II)} = \lambda_c^{(II)}(T)$ for various segments of the creep curve on T;
Dependences of the kinematic hardening module $g_1^c(T), g_2^c(T)$ on T.

The material parameters of the thermal creep equations are determined in basic experiments [, 27, 29].
Tests on uniaxial tension–compression of cylindrical laboratory specimens are considered as sic experiments the main types of which are isothermal experiments at constant base

MOST WIEDZY Downloaded from mostwiedzy.pl

temperatures T ($j = 1.2$ …). Using two types of specimens - continuous cylindrical and cylindrical tubular ensure a uniform distribution of stress strain fields and temperatures within the working part, excluding the possibility of loss of stability and shape change of the specimen under alternating loading as well as the effect of concentrators on SSS when moving from the working part of the specimen to thickened areas [27].

To determine the kinematic (anisotropic) hardening module $g_1^c(T)$ and $g_2^c(T)$ and the dependence for the creep surface radius corresponding to the zero creep rate, the specimen is heated to the temperature of the "basic" experiment $T = T_j = const$ and tests are carried out for short-term creep under uniaxial stress state according to the "soft" loading scheme.

First, the specimen is loaded up to the stress value $\sigma_{11}^{(1)}$ at the point 1 (Figure 5). This stress level is selected as a result of the analysis of the existing creep curve fan obtained at the "base" temperature $T = T_j$, (creep curve corresponds to zero creep rate). Due to relaxation the process end at point 2 (stress $\sigma_{11}^{(2)}$ where the creep strain rate tends to zero.

Further, the specimen is loaded up to the stress of reverse sign $\sigma_{11}^{(3)}$ (point 3 in Figure 5) and as a result of relaxation it appears in the point 4. Thus, stresses $\bar{\sigma}_{11}^{(0)+}$ (point 2) and $\bar{\sigma}_{11}^{(0)-}$ (point 4) characterize (with a certain tolerance for permanent strain) the initial upper and lower boundaries of the creep surface, corresponding to a zero creep rate.

To determine the transformation of creep surface on the same specimen at a specified stress $\sigma_{11}^* = const$a series of similar actions are carried out after reaching the assigned levels of creep deformations $e_{11}^{c(1)}, e_{11}^{c(2)}, \ldots, e_{11}^{c(m)}$. Thus obtained as set of points 2, 7, 12, 17, … characterizes the change in the upper (in tension) boundary of the creep surface as a function of accumulated creep strain. Points 4, 8, 13, 19, … characterize the change in the lower (under compression) boundary of the creep surface.

Thus, according to the results of the experiment at constant base temperatures $T = T_j$ we determine:

- Geometric location of the tensile creep strength with a specified tolerance for permanent deformation;
- Geometric location of the inverse creep strength under compression (Figure 6).

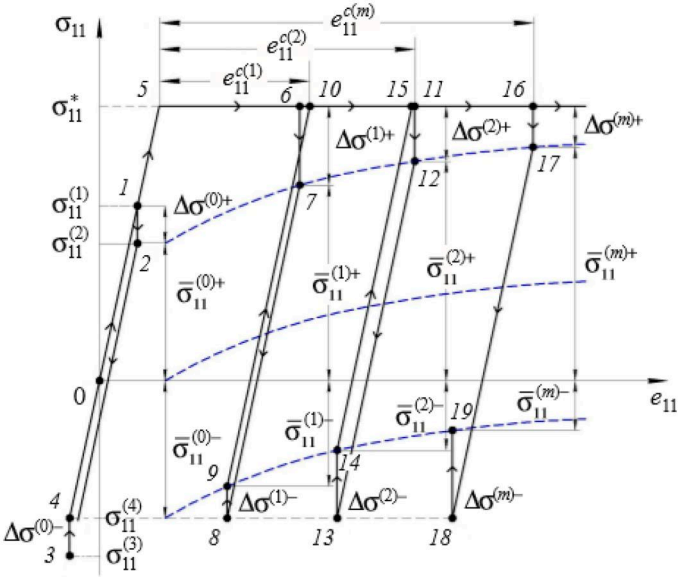

ure 5. Basic experiment as per scheme of soft loading.

MOST WIEDZY Downloaded from mostwiedzy.pl

The dependence of the creep surface radius corresponding to zero creep strain rate is determined by the formula:

$$\bar{C}_c = \sqrt{\frac{2}{3}}\frac{\sigma_{11}^{(m)+} + \sigma_{11}^{(m)-}}{2} \tag{20}$$

To determine the kinematic (anisotropic) hardening module $g_1^c(T)$ и $g_2^c(T)$ it is necessary to integrate the relation (8) at $T = T_j = const$

$$\rho_{11}^c = \frac{g_1^c}{g_2^c}(1 - e^{-g_2^c e_{11}^c}) \tag{21}$$

where e is natural logarithms base, g_1^c is the slope of the tangent to the curve $\rho_{11}{}^c \sim e_{11}{}^c$ at the origin (Figure 3), $\rho_{\max}^c = g_1^c/g_2^c$ is the asymptotic limit value ρ_{11}^c at a specified temperature $T = T_j$. Hence, we determine anisotropic (kinematic) hardening module g_1^c and g_2^c. For a uniaxial stress state of a laboratory specimen the ratios (1)–(18) take the form:

$$\sqrt{S_{ij}^c S_{ij}^c} - \bar{C}_c = \sqrt{\frac{2}{3}}\left(\sigma'_{11} - \frac{2}{3}\rho_{11}^c - \bar{\sigma}_c\right) \tag{22}$$

$$\dot{e}_{11}^c = \frac{2}{3}\lambda_c\left(\sigma'_{11} - \frac{3}{2}\rho_{11}^c - \bar{\sigma}_c\right) \tag{23}$$

where $\bar{\sigma}_c = \bar{\sigma}_c(e_{11}^c, T)$ the creep limit of the material corresponding to the zero creep rate

$$\dot{\chi}_c = \dot{e}_{11}^c, \chi_c = e_{11}^c \tag{24}$$

$$\bar{C}_c = \sqrt{\frac{2}{3}}\bar{\sigma}_c \tag{25}$$

Parameters $\lambda_c^{(0)}$ and $\lambda_c^{(II)}$ are derived from relations (21) and (22), respectively

$$\lambda_c^{(0)} = \frac{3}{2}\frac{\dot{e}_{11}^{c(H)}}{\sigma'_{11} - \bar{\sigma}_c} \tag{26}$$

$$\lambda_c^{(II)} = \frac{3}{2}\frac{\dot{e}_{11}^{c(Y)}}{\sigma'_{11} - (3/2)\rho_{11}^c - \bar{\sigma}_c} \tag{27}$$

where $\dot{e}_{11}^{c(H)}$ is initial creep strain rate at a point $e_{11}^c = 0$ on the curve $e_{11}^c(t), \dot{e}_{11}^{c(Y)}$ is creep strain rate in the region of steady-state creep (region II in Figure 4).

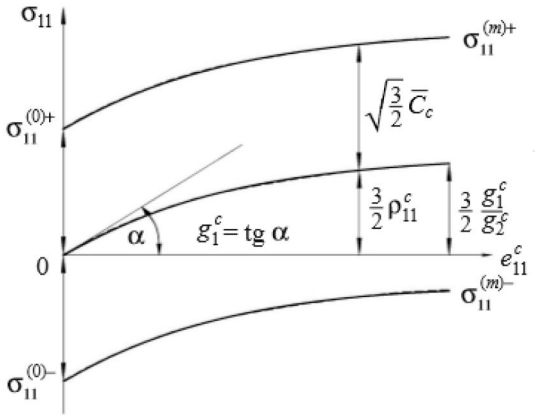

ure 6. Geometric location of creep limits under tension and compression.

MOST WIEDZY Downloaded from mostwiedzy.pl

The material parameters of the evolutionary equations of damage accumulation were experimentally determined at the second stage of damage accumulation process, from which the significant effect of damage on the physical mechanical properties of material begins. The experimental deformation processes have been simultaneously calculated at this stage using the thermo viscoplasticity relations. In fact, the technique involves all deviations in the results of numerical modeling of deformation processes without accounting for the effect of damage from the experimental ones at the second stage of damage accumulation are attributed to the effect of damage ω (decrease in the elastic modulus and stress amplitude at a constant strain amplitude, an increase in the strain amplitude at a constant stress amplitude and etc.).

The boundaries W_c^a and W_c^f can be approximately determined from creep tests at a specified stress amplitude by the time of material softening (W_c^a determined by the beginning of the second section of the creep curve, while W_c^f by the moment of macroscopic crack formation).

Tables 1 and 2 show the material parameters of the VT6 titanium alloy at a temperature of 600 °C for the mathematical creep model given in this article.

5. Numerical results and their comparison with experimental data

Figures 7–12 present the results of tension and torsion tests for short-term creep as per the test program shown in Figure 3. Here, solid lines indicate the results of numerical modeling of experimental processes using the constitutive relations of MDM (1)–(19), and markers indicate the corresponding experimental data.

Figures 13 and 14 present the results of short-term creep tests under multiaxial stress state (torsional tension) according to the test program shown in Figure 3. Solid lines indicate the results of numerical modeling, markers indicate the corresponding experimental data.

Comparing the obtained experimental data with the results of numerical modeling of experimental processes, we can note their qualitative and quantitative coincidence. Some differences between the calculated and experimental data can be explained by inaccuracy in setting material parameters and scalar functions due to the lack of statistic scattering of the experimental data.

6. Conclusion

A mathematical model of MDM is developed that describes the processes of unsteady creep and long-term strength of structural materials (metals and their alloys) under multiaxial stresses.

Table 1. Material parameters of the mathematical model of creep.

Bulk modulus K, MPa	62,855
ar modulus G, MPa	29,010
ep coefficient λ_c^0, 1/ MPa·h	0.00060
ady-state creep coefficient λ_c^{II}, 1/ MPa·h	0.00031
teady creep length $\chi_c^{(1)}$	0.005
ematic hardening modulus g_1^c, MPa	1100
ematic hardening modulus g_2^c, MPa	49.55
energy of the end of the first stage of damage accumulation W_c^a, MJ/m^3	4.00
ep failure energy W_c^f, MJ/m^3	19.0
o-level creep surface radius C_c, MPa	15.0
erial parameter k	1

le 2. The zero-level creep surface radius as a function of the path length of plastic deformation.

	0	0.03	0.04	0.06	0.08	0.10	0.12	0.14	0.16	0.20
MPa	15.0	15.0	14.9	14.7	14.5	13.0	8.50	3.75	2	2

MOST WIEDZY Downloaded from mostwiedzy.pl

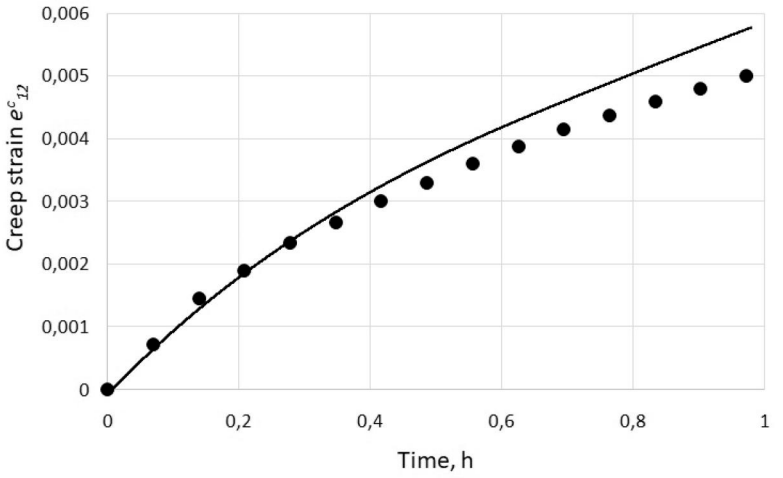

Figure 7. Torsion creep curve (loading scheme "a").

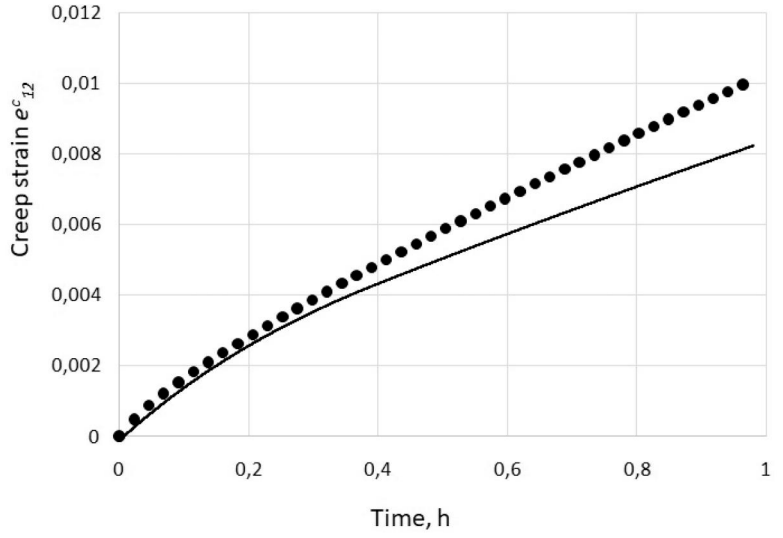

Figure 8. Torsion creep curve (loading scheme "b").

An experimental–theoretical technique is elaborated for determining material parameters and lar functions of the proposed constitutive relations of MDM. The material parameters of con- utive relations for thermal creep for VT6 titanium alloy at a temperature of 600 °C are tained.

Experimental studies of high-temperature creep of VT6 titanium alloy under uniaxial and ıltiaxial stresses are carried out. The results of numerical modeling of experimental processes compared with experimental data. It is shown that the developed version of the constitutive ations of MDM allows us to describe the processes of unsteady creep and long-term strength structural alloys under uniaxial and multiaxial stresses with accuracy sufficient for engineering culations.

MOST WIEDZY Downloaded from mostwiedzy.pl

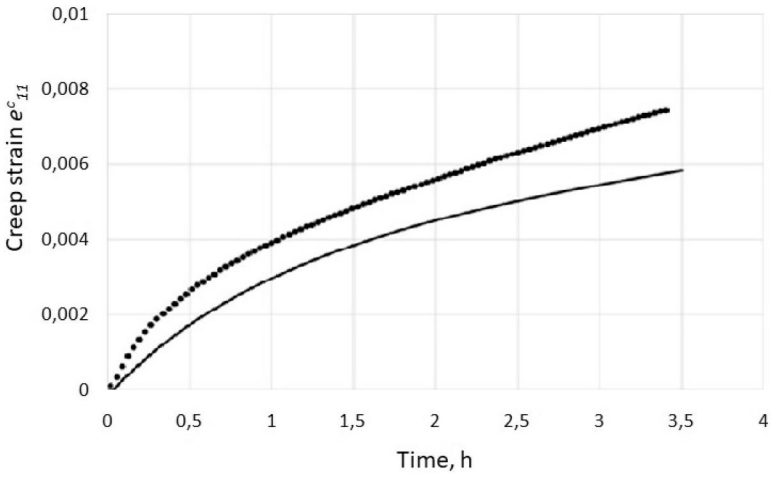

Figure 9. Tensile creep curve (loading scheme "c").

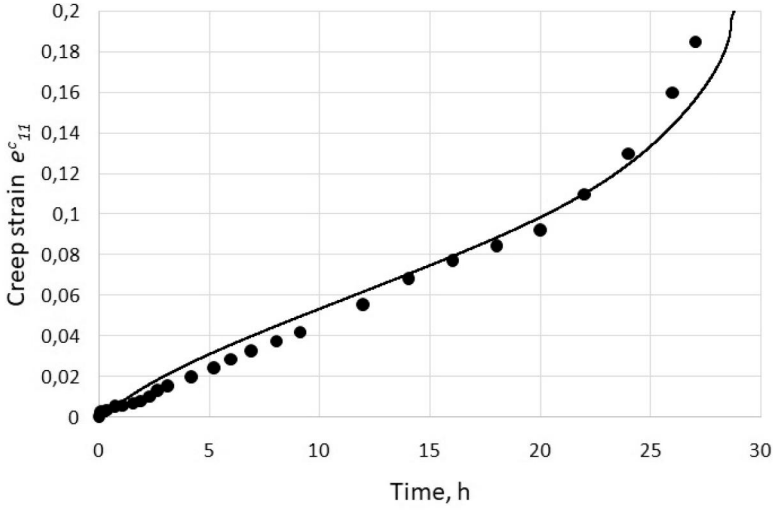

Figure 10. Tensile creep curve (loading scheme "d").

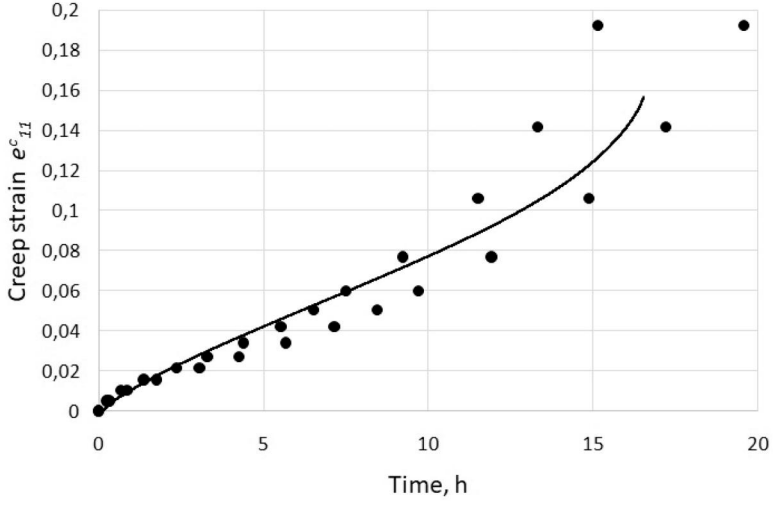

ure 11. Tensile creep curve (loading scheme "e").

MOST WIEDZY Downloaded from mostwiedzy.pl

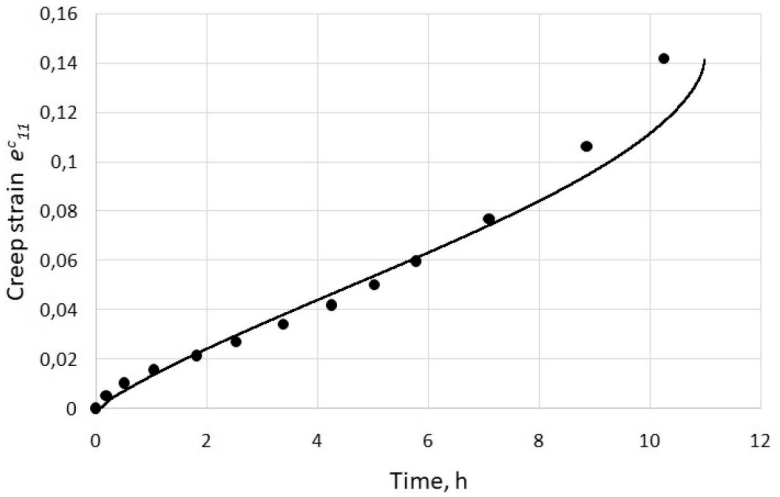

Figure 12. Tensile creep curve (loading scheme "f").

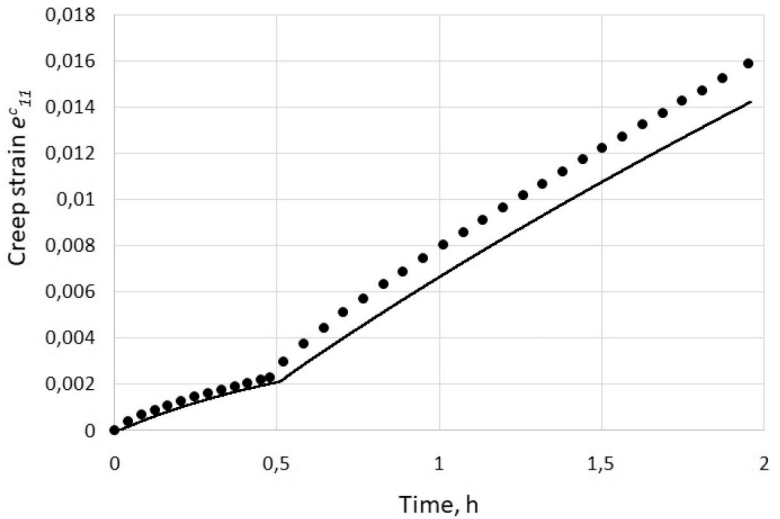

Figure 13. Axial deformation e^c_{11} as a function of process time (loading scheme "g").

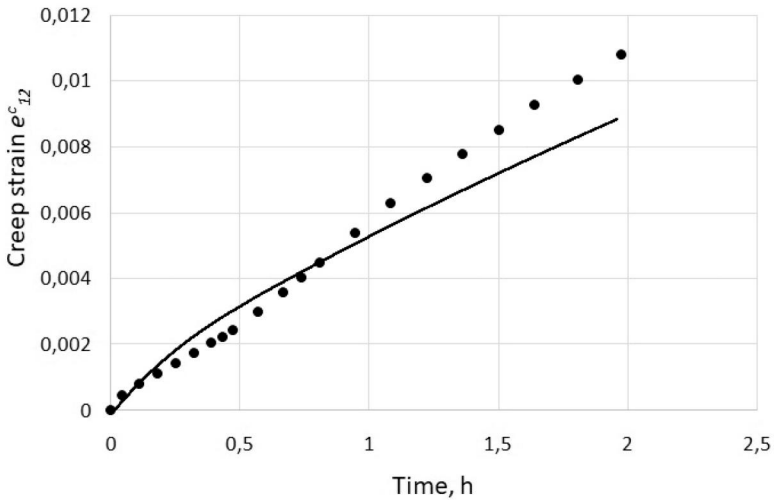

Figure 14. Shear deformation e^c_{12} as a function of process time (loading scheme "h").

MOST WIEDZY Downloaded from mostwiedzy.pl

Disclosure statement

No potential conflict of interest was reported by the author(s).

Funding

The work was carried out with the financial support of the Ministry of education (Task 0729-2020-0054) in terms of experimental research and Scientific and Russian Science Foundation (Grant No. 22-19-00138) in terms of numerical calculations.

ORCID

Leonid A. Igumnov http://orcid.org/0000-0003-3035-0119
Ivan A. Volkov http://orcid.org/0000-0003-1176-4906
Denis N. Shishulin http://orcid.org/0000-0002-6527-557X
Ivan A. Modin http://orcid.org/0000-0002-3561-4606
Aleksandr A. Belov http://orcid.org/0000-0003-3704-048X
Victor A. Eremeyev http://orcid.org/0000-0002-8128-3262

References

[1] J. A. Collins, *Faillure of Materials in Mechanical Design: Analysis, Prediction, Prevention*. New York: Wiley-Interscience Publication; 1981.

[2] K. Naumenko and H. Altenbach, *Modeling of Creep for Structural Analysis*. Berlin, Germany: Springer Science & Business Media; 2007.

[3] R. A. Dul'nev and P. I. Kotov, *Termicheskaya Ustalost' Metallov [Thermal Fatigue of Metals]*. Moscow, Russia: Mashinostroenie Publishers; 1980 (In Russian).

[4] L. A. Igumnov, D. A. Kazakov, D. N. Shishulin, I. A. Modin and D. V. Zhegalov, "Experimental studies of high-temperature creep of titanium alloy VT6 under conditions of a complex stress state under the influence of an aggressive medium," *Vestnik Samarskogo Gosudarstvennogo Tekhnicheskogo Universiteta, Seriya Fiziko-Matematicheskie Nauki*, vol. 25, no. 2, pp. 286–302, 2021. DOI: 10.14498/vsgtu1850.

[5] A. G. Kazantsev, Issledovanie vzaimodeystviya malotsiklovoy ustalosti i polzuchesti pri neizotermicheskom nagruzhenii [Investigation of the interaction of low-cycle fatigue and creep under non-isothermal loading]. Problemy prochnosti [Strength of Materials]; 1985, No 5., pp. 25–31 (In Russian).

[6] I. A. Volkov and Y. Korotkikh, *Uravneniya sostoyaniya vyazkouprugoplasticheskikh sred s povrezhdeniyami [State Equations for Viscoelasticoplastic Media with Injuries]*. Moscow, Russia: Fizmatlit Publishers, 2008 (In Russian).

[7] J. T. Boyle and J. Spence, *Stress Analysis for Creep*. London: Butterworths; 1980.

[8] V. P. Degtyarev, *Plastichnost' i polzuchest' mashinostroitel'nykh konstruktsiy [Plasticity and Creep of Engineering Structures]*. Moscow, Russia: Mashinostroenie Publisher; 1967 (In Russian).

[9] D. A. Gokhfel'd and O. S. Sadakov, *Plastichnost' i Polzuchest' Elementov Konstruktsiy Pri Povtornykh Nagruzheniyakh [Plasticity and Creep of Structural Elements under Repeated Loading]*. Moscow, Russia: Mashinostroenie Publishers; 1984 (In Russian).

] A. M. Lokoshchenko, *Polzuchest' i Dlitel'naya Prochnost' Metallov [Creep and Long Durability of Metals]*. Moscow, Russia: Fizmatlit Publishers; 2016 (In Russian).

] N. N. Malinin, *Prikladnaya Teoriya Plastichnosti i Polzuchesti [Applied Theory of Plasticity and Creep]*. Moscow, Russia: Mashinostroenie Publishers; 1968 (In Russian).

] N. N. Malinin and G. M. Khadjinsky, "Theory of creep with anisotropic hardening," *Int. J. Mech. Sci.*, vol. 14, no. 4, pp. 235–246, 1972. DOI: 10.1016/0020-7403(72)90065-3.

] A. Miller, "Mathematical model for monotonous and cyclic variation of deformation and creep deformation," *ASME, Series D. Theoretical Foundations of Engineering Calculations*, no. 2, pp. 1–20, 1976.

] N. Rabotnov Yu, *Polzuchest' Elementov Konstruktsiy [Creep of Structural Elements]*. Moscow, Russia: Nauka Publishers; 1966 (In Russian).

] V. S. Bondar, *Neuprugost'. Varianty Teorii [Inelasticity. Variants of the Theory]*. Moscow, Russia: Fizmatlit Publishers; 2004 (In Russian).

] J. L. Chaboche, "Constitutive equation for cyclic plasticity and cyclic viscoplasticity," *Int. J. Plasticity*, vol. 5, no. 3, pp. 247–302, 1989. DOI: 10.1016/0749-6419(89)90015-6.

MOST WIEDZY Downloaded from mostwiedzy.pl

[17] R. D. Krieg, J. C. Swearengen and R. W. Rohde, "A physically-based internal variable model for rate-dependent plasticity," in *Proceeding of the Conference "Inelastic Behavior of Pressure Vessel and Piping Components"*, T. Y. Chang and E. Krempl , Eds. ASME; 1978, pp. 245–271

[18] I. A. Modin, A. V. Kochetkov, N. V. Leontev, I. A. Turigina and E. Y. Poverennov, "Numerical modeling of nonlinear dynamic and static compression of the metal mesh," *PNRPU Mech. Bull.*, vol. 4, pp. 106–113, 2019. DOI: 10.15593/perm.mech/2019.4.10.

[19] P. Perzyna, *Osnovnye Voprosy Vyazkoplastichnosti [Fundamental Problems in Viscoplasticity]*. Moscow, Russia: Mir Publishers; 1968 (In Russian).

[20] N. Shevchenko Yu and R. G. Terekhov, *Fizicheskie uravneniya termovyazkoplastichnosti [Physical Equations of Thermoviscoplasticity]*. Kiev, Ukraine: Naukova Dumka Publishers; 1982 (In Russian).

[21] I. A. Volkov, L. A. Igumnov and G. Korotkikh Yu, *Prikladnaya teoriya vyazkoplastichnosti [Applied Theory of Viscoplasticity]*. Nizhni Novgorod, Russia: NNGU Publishers, 2015. (In Russian).

[22] V. V. Balandin, A. V. Kochetkov, S. V. Krylov and I. A. Modin, "Numerical and experimental study of the penetration of a package of woven metal grid by a steel ball," *J. Phys.: Conf. Ser.*, vol. 1214, no. 1, pp. 012004, 2019. DOI: 10.1088/1742-6596/1214/1/012004.

[23] I. A. Modin, A. V. Kochetkov and N. V. Leontiev, "Numerical simulation of quasistatic and dynamic compression of a granular layer," *AIP Conf. Proc.*, vol. 2116, p. 270003, 2019. DOI: 10.1063/1.5114277.

[24] Y. Ohashi, N. Ohno and M. Kawai, "Evaluation of creep constitutive equations for type 304 stainless steel under repeated multiaxial loading," *ASME J. Eng. Mater. Technol.*, vol. 104, pp. 159–164, 1982.

[25] D. A. Kazakov, S. A. Kapustin and G. Korotkikh Yu, Modelirovanie processov deformirovaniya i razrusheniya materialov i konstrukcij [Modeling the processes of deformation and failure of materials and structures]. Izdatel'stvo Nizhegorodskogo Universiteta, N.Novgorod, Russia; 1994 (In Russian).

[26] I. A. Volkov, V., *et al.*, "Model' povrezhdennoj sredy dlya opisaniya dlitel'noj prochnosti konstrukcionnyh materialov (metallov i ih splavov) [Damaged medium model for describing the long-term strength of structural materials (metals and their alloys)]," *PSP*, vol. 79, no. 3, pp. 285–300, 2017 (In Russian). DOI: 10.32326/1814-9146-2017-79-3-285-300.

[27] A. V. Kochetkov, N. V. Leontev, I. A. Modin and A. O. Savikhin, Nizhny Novgorod, Russian Federation., "Study of the stress-strain and strength properties of the metal woven grids," *Tomsk State Univ. J. Math. Mech.*, vol. 52, no. 52, pp. 53–62, 2018. DOI: 10.17223/19988621/52/6.

[28] I. A. Volkov and L. A. Igumnov, *Vvedenie v Kontinual'nuyu Mekhaniku Povrezhdennoj Sredy [Introduction to the Continuum Mechanics of Damaged Medium]*. Moscow, Russia: Fizmatlit Publishers; 2017 (In Russian).

[29] I. A. Volkov, L. A. Igumnov, I. A. Modin and E. V. Boev, "A model of damaged media for describing a creep-induced damage accumulation process. 9th International Conference on Materials Structure and Micromechanics of Fracture," *Procedia Struct. Integrity*, vol. 23, pp. 281–286, 2019. DOI: 10.1016/j.prostr.2020.01.100.

MOST WIEDZY Downloaded from mostwiedzy.pl